

High-speed growth of TiO₂ nanotube arrays with gradient pore diameter and ultrathin tube wall under high-field anodization

This article has been downloaded from IOPscience. Please scroll down to see the full text article.

2010 Nanotechnology 21 405302

(<http://iopscience.iop.org/0957-4484/21/40/405302>)

View [the table of contents for this issue](#), or go to the [journal homepage](#) for more

Download details:

IP Address: 202.120.52.96

The article was downloaded on 22/10/2010 at 09:13

Please note that [terms and conditions apply](#).

High-speed growth of TiO₂ nanotube arrays with gradient pore diameter and ultrathin tube wall under high-field anodization

Xiaoliang Yuan^{1,2}, Maojun Zheng^{1,2,4}, Li Ma³ and Wenzhong Shen^{1,2}

¹ Key Laboratory of Artificial Structures and Quantum Control, Ministry of Education, Department of Physics, Shanghai Jiao Tong University, Shanghai 200240, People's Republic of China

² Laboratory of Condensed Matter Spectroscopy and Opto-Electronic Physics, Department of Physics, Shanghai Jiao Tong University, Shanghai 200240, People's Republic of China

³ School of Chemistry and Chemical Technology, Shanghai Jiao Tong University, Shanghai 200240, People's Republic of China

E-mail: mjzheng@sjtu.edu.cn

Received 19 June 2010, in final form 10 August 2010

Published 10 September 2010

Online at stacks.iop.org/Nano/21/405302

Abstract

Highly ordered TiO₂ nanotubular arrays have been prepared by two-step anodization under high field. The high anodizing current densities lead to a high-speed film growth (0.40–1.00 μm min⁻¹), which is nearly 16 times faster than traditional fabrication of TiO₂ at low field. It was found that an annealing process of Ti foil is an effective approach to get a monodisperse and double-pass TiO₂ nanotubular layer with a gradient pore diameter and ultrathin tube wall (nearly 10 nm). A higher anodic voltage and longer anodization time are beneficial to the formation of ultrathin tube walls. This approach is simple and cost-effective in fabricating high-quality ordered TiO₂ nanotubular arrays for practical applications.

(Some figures in this article are in colour only in the electronic version)

1. Introduction

In recent years, nanotubular materials have attracted increasing attention due to their unique properties and potential applications [1–3]. The different chemical and physical properties of these novel materials have been ascribed to their characteristic structural features, that is, high surface-to-volume ratios and size-dependent properties. In particular, much more recent studies have indicated that ordered TiO₂ nanotube arrays possess outstanding charge transport properties. So this outstanding properties had enabled a variety of advanced applications in gas sensing [4], dye-sensitized solar cells [5–10], catalysis [11–14], doping [15], biomedicine [16] and photovoltaics [17–19]. In recent years, there have been many reports on the synthesis strategies of

nanotubular TiO₂ film structures already, such as template-based methods [20, 21], hydrothermal processes [22, 23], sol-gel transcription using organo-gelators as templates [24, 25], electroless deposition methods [26] and anodic oxidation of titanium [27–31]. However, of all these methods, anodic oxidation is considered as the most prominent one, in which the dimensions can be precisely controlled.

Fabrication of TiO₂ nanotube arrays via anodic oxidation was first reported in 2001 by Grimes *et al* [27] using titanium foil in a fluoride-based electrolyte. They had reported that the composition of the electrolyte determined both the rate of nanotubular array formation, as well as the rate of the resultant oxides' dissolution. In the electrolytes, fluoride ions play an important role in the nanotubular array formation rather than other components. And in recent years, precise control of the nanotube morphology [27] and parameters of dimensions, such

⁴ Author to whom any correspondence should be addressed.

as length, pore size [28] and wall thickness [32], have been studied.

For the HF-based electrolyte (0.5 wt% HF aqueous solution) [27, 33–35], foils were anodized at lower voltages, varying from 3 to 20 V at room temperature. It was found that at a lower voltage the porous film is similar to that of porous Al₂O₃ [36]. As the voltage increased to 10 V or even larger, the discrete, hollow, cylindrical tube-like features gradually appeared. However, these layers showed a limited thickness that would not exceed 500–600 nm. Later, Macak *et al* [30, 37–39] carried out a series of experiments using a buffered neutral KF-based (or NaF-based) aqueous electrolyte system with variable pH and got improved nanostructured arrays. In this strongly acidic solutions (pH < 1), they got nanotubular structures at anodization voltages larger than 25 V. As the conditions of this system are strongly determined by pH, that means longer nanotubes can be formed in lower pH solutions. They had got nanotubes with layer thicknesses greater than 2 μm . Meanwhile, another group chose an organic electrolyte (nonaqueous solution) [40] and they had got tubes with extremely smooth walls and tube lengths exceeding 7 μm . After that, Grimes and his co-workers reported in 2006 the use of polar organic solvents such as dimethyl sulfoxide (DMSO), ethylene glycol, formamide and *N*-methyl formamide to achieve nanotube arrays with lengths of several hundred microns [41]. Subsequently they prepared nanotube arrays up to 1005 μm in length [42]. Paulose *et al* [43] used an electrolyte composition of 0.3 wt% NH₄F and 2 vol% H₂O in ethylene glycol and the anodization voltage was 60 V. The inner diameter was about 90 nm, wall thickness was about 50 nm, the distance between holes could reach up to 150–200 nm and the anodization time lasted for 72 h, which was considered to be much longer for the optimum anodizing conditions to achieve optimal arrays.

So far, many more studies on the fabricating technology of TiO₂ nanotube arrays via anodic oxidation were done at relatively lower fields (5–60 V) [44, 45]. Precise control of the nanotubes' wall thickness and the tube-to-tube spacing are still huge challenges. Here, we report the fabrication of TiO₂ nanotube arrays with gradient diameters and ultrathin tube walls (~10 nm) by two-step high-field anodization and then thermal annealing approaches. The distance between holes could be controlled on a large scale and the growth rate of the layer could also be enhanced greatly, which means a shortened time of anodization (4 h).

2. Experimental details

Prior to our anodization, the titanium foils (99.7% purity) or annealed titanium foils (at 800 °C in an argon atmosphere) with a radius of 1 cm and about 0.25 mm thickness should be polished. First, the foils were degreased in acetone for 10 min and then ultrasonically cleaned in distilled water. Then the foils were dried in air for about 3 h. Finally, a chemical polish (15 min) was finished in HF (4 vol%). This was the key step in our pre-experiments, which determined the surface status of the titanium foils. The polished titanium foils were then put into a tailor-made holder with a circular area of 2 cm² exposed to the electrolyte.

Table 1. Parameters of the two-step anodization at different voltages and times.

	90 V	120 V	150 V	180 V	220 V
Anodization temperature (°C)	20	20	0	0	−10
Anodization time (min)	240	120	120	120	20
Growth rate of the layer ($\mu\text{m min}^{-1}$)	0.42	0.97	0.80	0.93	0.94

A two-electrode (a Pb board as cathode, titanium foils as anode), temperature-controlled (20, 0 and −10 °C) electrochemical anodization bath was used. A stirring apparatus (800 rpm) was used to make sure that the reaction occurred in a uniform electrolyte. A regulated DC power supply (AgilentN5752A) was used to ensure a uniform local voltage.

For the whole fabrication process, we used an electrolyte composition of 0.3 wt% ammonium fluoride (NH₄F) and 4 vol% water in ethylene glycol (96 vol%). Anodization was carried out at three temperatures (20, 0 and −10 °C), different voltages and times (shown in table 1).

After the anodization, we dried our resulting samples (the oxide layer adheres to the titanium foils) in air at room temperature for 24 h. Then the oxide layer would be isolated from the titanium foils automatically. Next, we used the remaining titanium foils as a new anode. The following operation was the same as before. We called this method two-step oxidation. Highly ordered TiO₂ nanotubular arrays were fabricated through this two-step anodizing electrochemical procedure.

The TiO₂ nanotubular arrays were further annealed at different temperatures (400 and 800 °C) to get different crystalline structures (anatase and rutile phases).

The morphologies of our samples made by two-step oxidation were observed using a field-emission scanning electron microscope (FESEM, Philips XL30FEG). Energy-dispersive x-ray (EDX) spectroscopy (INCA Oxford) was recorded at the surface of the pre-texture titanium foil (made by removing the TiO₂ layer of the first step of anodization). Crystal structures of two different titanium foils were examined using x-ray diffraction (Lab XRD-6000, Shimadzu).

3. Results and discussion

Figure 1(a) shows the SEM image of TiO₂ nanotubular arrays through the one-step oxidation. However, there is a thin layer with irregular holes on the tubular structure and the TiO₂ nanotubes are not dispersed, while it is noticed that the whole oxide layer can be isolated from the titanium foils automatically when the anodization time is about 4 h after drying in air for some time, as shown in figure 1(b). Next we observed the backside of the oxide layer. Unfortunately, in this one-step oxidation, the barrier layers with a thickness of about 0.5 μm were not separated from the tube layers completely.

In particular, it was observed that the surface of titanium foil without an oxide layer has a honeycomb structure (each cell is actually an etch pit, as shown in figure 1(c)). Furthermore, EDX spectroscopy of the surface of the

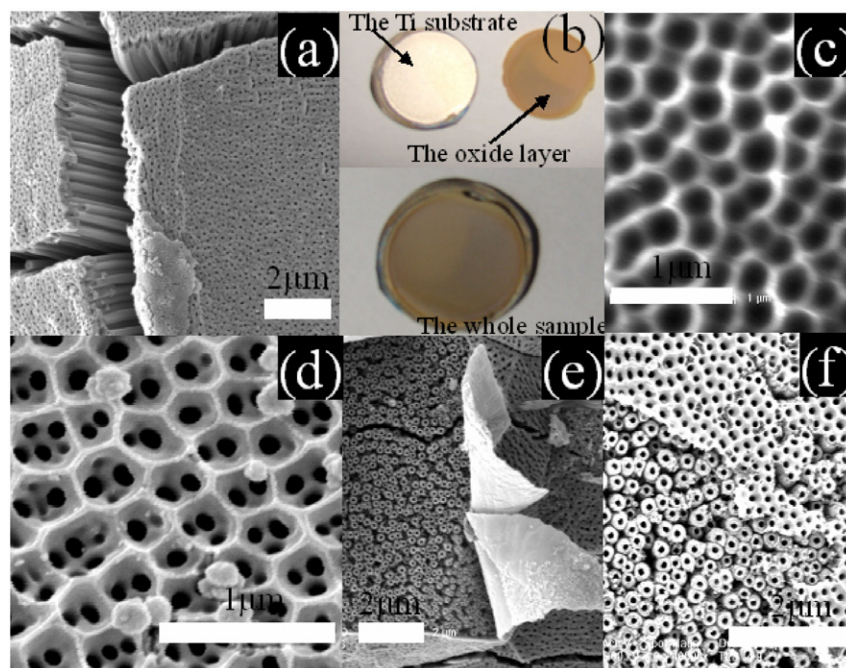


Figure 1. FESEM images and photo images of anodic TiO₂ membranes. (a) One-step anodization at 90 V; (b) the titanium substrate after the whole oxide layer was isolated automatically, free-standing TiO₂ membranes and as-prepared whole sample; (c) the surface of titanium substrate after TiO₂ membrane breaking off; (d) and (e) TiO₂ nanotubular array membrane prepared by second anodization at 90 V; (f) TiO₂ nanotubular array membrane prepared by second anodization at 180 V.

honeycomb structure indicated that its chemical composition is only Ti. The honeycomb structure would act as a pre-texture layer in the later anodization for obtaining high-quality TiO₂ nanotubular arrays based on the idea of two-step oxidation used in fabricating porous anodic alumina [46]. However, the whole two-step anodization was different from the synthesis of alumina films using a multi-step anodization process (their substrate and oxide layer were not separated) [47]. Then the etch pits on the titanium foils acted as new growth points for the second step of anodization. As the anodization proceeded gradually, the radius of each etch pit became larger. We could see pentagonal, polygonal and hexagonal pores in an alternating arrangement, and a brand-new tubular structure was obtained, as shown in figure 1(d). Each etch pit contained several small pores and the ultrathin layer did not match with the tube layer very well. However, when we increased the anodization voltage to 180 V, the pores of the cover layer matched with the tube layer. Fortunately, the etch pits only acted as new growth points and there were quite large inner stresses which would lead to the separation of these two layers if we dry the membrane in air at room temperature for some time, as shown in figures 1(e) and (f). All of our membranes fabricated at different voltages (90–220 V) via two-step oxidation display the same phenomenon. The different tube diameters from 200 to 280 nm can be obtained by changing the anodic voltage.

As we know, a good single tube should possess three features: ultrathin tube wall, large diameter and the length as large as possible. Paulose *et al* reported the fabrication of nanotube arrays up to 1005 μm in length [42]. At the same time, they also produced better results for improved tube wall

and diameter [43]. It has been found that the annealing method is a effective approach for obtaining the single dispersive and ultrathin tube wall TiO₂ nanotube arrays in our experiment. Figure 2 shows the surface SEM image of a nanotubular array membrane made from annealed titanium foils. We observed that the wall thickness, which was determined by anodization time and voltage, is quite small and nearly 10 nm, compared to that of the ordinary tubular membrane made from unannealed titanium foils. For the process at 90 V (figure 2(a)), the anodization time is much longer than that at 180 V (figure 2(b)), so the thickness of the tube wall is smaller. However, the thickness also decreases when we increase the voltage to 220 V, as shown in figure 2(c). Furthermore, cross-sectional images (figure 3) also indicate that the nanotubes are uniform and their tube walls are ultrathin and smooth. The pore diameter reveals obviously a gradient variation along the tube from the surface to the end (figure 3(c)). We could reach the conclusion that a higher voltage and longer anodization time will lead to an ultrathin tube wall. However, the voltage should not be very large in case of burning out the electrode. Interestingly, there is a hat-like barrier layer on the backside of the membrane, as shown in figure 4. Also, the barrier layer would detach automatically, leaving monodisperse and double-pass tubes. We can see clearly that the inner diameter of the tube on the backside does not equal that on the surface. This also proved that the inner structure of a single tube was V-like. The schematic representation of the double-pass tubes without a barrier layer is shown in figure 5. However, the removal of the barrier layer would lead to different features on the backside of the membrane. During the anodization, reaction heat dissipation in the electrolyte was not uniform, which

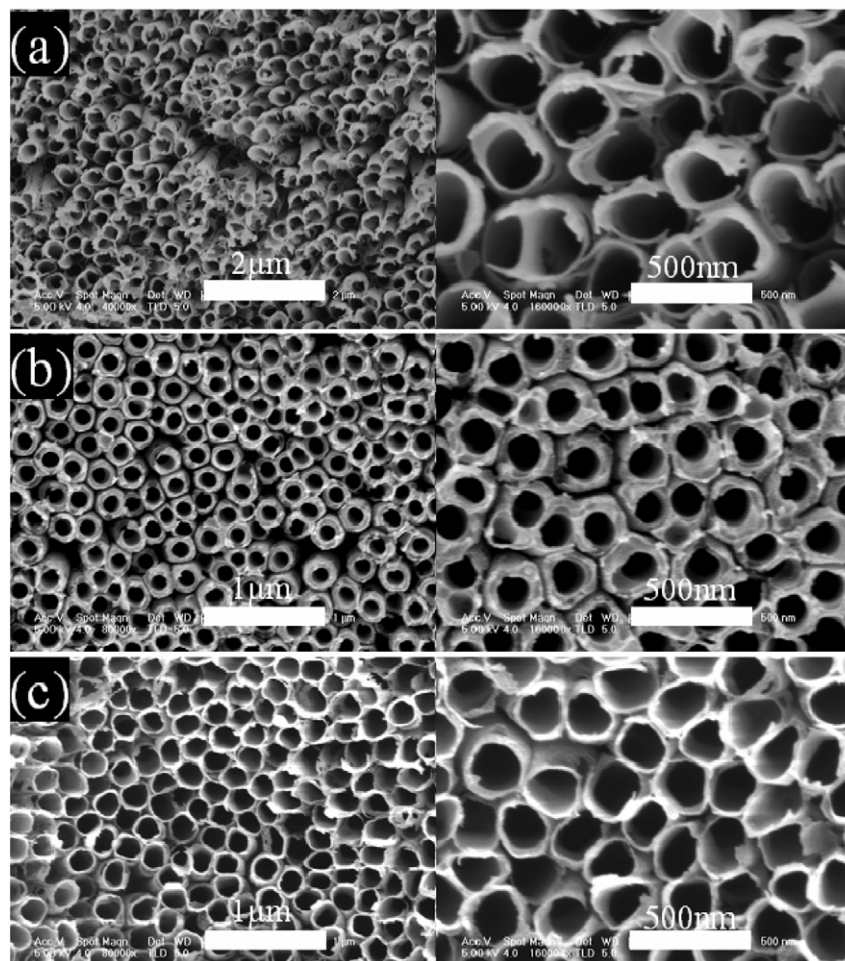
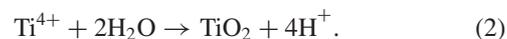


Figure 2. FESEM images of TiO₂ nanotubular array membrane made from annealed titanium foils at different anodic voltages (the right is at higher magnification). (a) 90 V, (b) 180 V and (c) 220 V.

led to unsmooth surface conditions. Hence, the thickness of the barrier layer was variable in different areas and we could just get various structures on the backside, such as funnel-formed structures (figure 4(b)) and typical acclinic structures (figure 4(c)). The formation of these structures was greatly affected by adhesive forces of the barrier layer. If the adhesive forces are too large they destroy the typical acclinic structures at the surface and we get multilayer structures, as shown in figure 4(d).

The growth mechanism of TiO₂ nanotubes can be explained based on the current–time ($I-t$) curves (figure 6). During the experiment, the current–time curves were recorded during each step of anodization. It was found that the $I-t$ curves revealed a similar changing trend at different steps (the first and the second anodization), different anodic voltages (90–220 V) and different titanium foils (annealed or unannealed). Hence, $I-t$ curves at the first step (figure 6(a)) can be used to explain the synthesis of the common TiO₂ nanotube films. The current decreased sharply initially, followed by a rapid increase, and then the current stayed relatively stable, as seen from figure 6. In this $I-t$ curves, regions I and II are defined as unsteady states, and region III is steady state. After stage III, the films would grow at a uniform rate. During the initial period of anodization, a compact

high-resistant oxide film (the barrier layer) was formed on the titanium substrate and the current decreased rapidly with time. This initial stage could be described by these two equations, including the fast dissolution of titanium and a little formation of oxide [48, 49]:



At 10 s, the current decreased to the minimum. At the minimum of the current, a propagation of individual paths through the barrier layer began and an increase in the current density was observed. As a result of that, pore precursors were formed. In stage II, the current began to increase and maintained growth due to the effect of the high electric-field is assisting the dissolution of titania. Also, this stage could be described using a chemical reaction equation:



After 40 s or so (stage III), the current did not change significantly with time since it reached the maximum dissolution rate of titania at the bottom of the nanotubes and the porous oxide layer started to grow on titanium. In this stage, there was a dynamic equilibrium between the formation

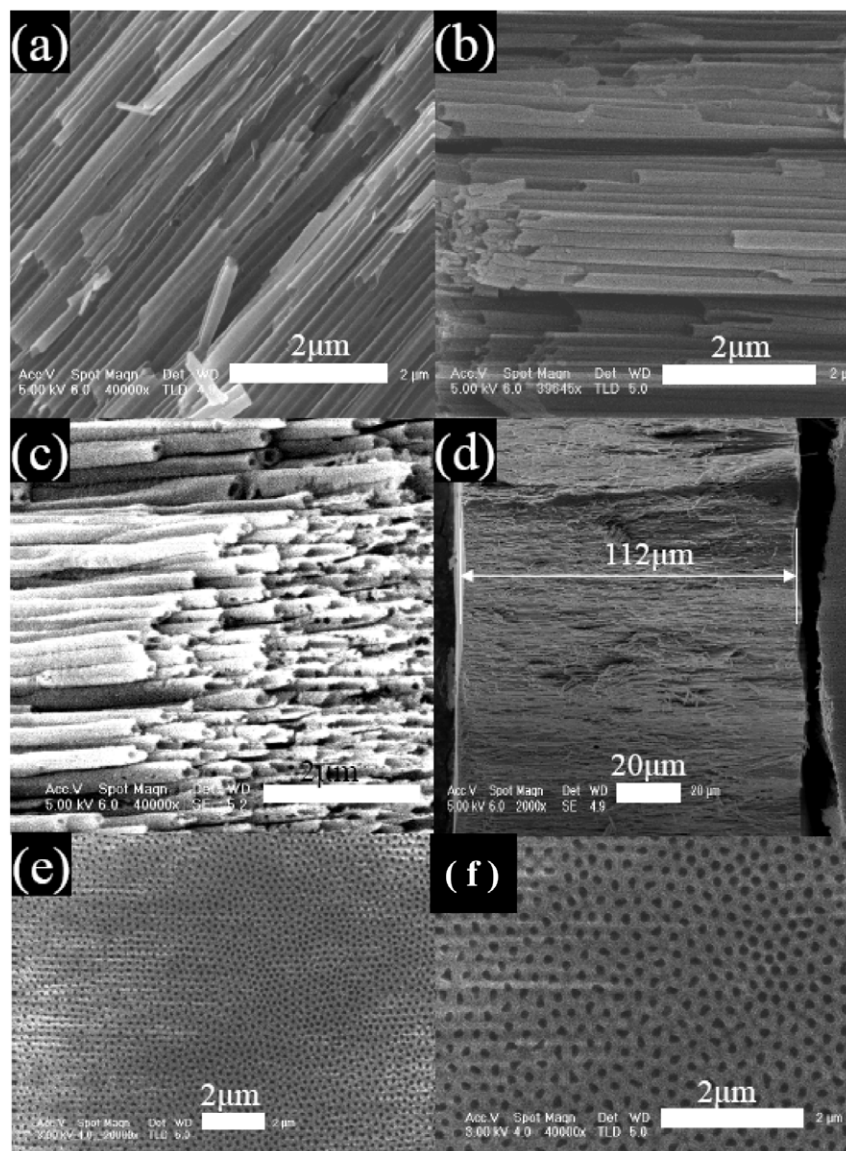


Figure 3. Cross-sectional FESEM images of TiO₂ nanotubular array membrane made from annealed titanium foils at different voltages: (a) 90 V; (b) 180 V; (c) 220 V; (d) the whole cross-sectional image of the film at 180 V; (e) surface FESEM images of TiO₂ nanotubular array membrane made from annealed titanium foils at the first step of anodization; (f) the higher magnification of (e).

and dissolution of titania, that is the growth rate of the oxide layer equals that of oxide dissolution. But the barrier layer still adheres to the oxide layer and moves deeper into the metal without any change and made the pore also deeper at the same time. A higher-field anodization will lead to a much thicker oxide layer. Interestingly, these processes were quite similar to those of alumina [50, 51].

As the time of the unsteady states is too short (10 s) compared to the steady state (20 min or more), we only use the time of the steady state as the growth time. The growth rate (R) can be calculated using the formula $R = h/t$. Here h means the thickness of the film, which could be measured from SEM morphology (figure 3(d)), and t is the growth time. The growth rates at each voltage were shown in table 1. In our experiments, growth rate of the membranes varied from 0.40 to 1.00 $\mu\text{m min}^{-1}$ when the anodization voltages varied from

90 to 220 V. The growth rate in our experiments has improved greatly and nearly 16 times as much as in traditional fabrication ($0.0625 \mu\text{m min}^{-1}$, 360 μm for 96 h) of TiO₂ at low field [42].

The formation of a V-like structure with ultrathin tube wall TiO₂ nanotube arrays by using annealed titanium foils should be due to the change in microstructure of the foil. We examined two titanium foils by x-ray diffraction, shown in figure 7. The peak intensity of the annealed titanium is a bit weaker than that of the unannealed one and there is very little amount of rutile TiO₂ mixed with Ti. Hence, the granulation process occurs in the whole titanium foils during the annealing, and titanium atoms could be activated due to high surface area, which will be beneficial to the fast dissolution of titanium (reaction (1)). This will result in the generation of a larger current during anodization, which will lead to the formation of high-quality ordered pore films [46]. Figures 3(e) and (f) show that the film

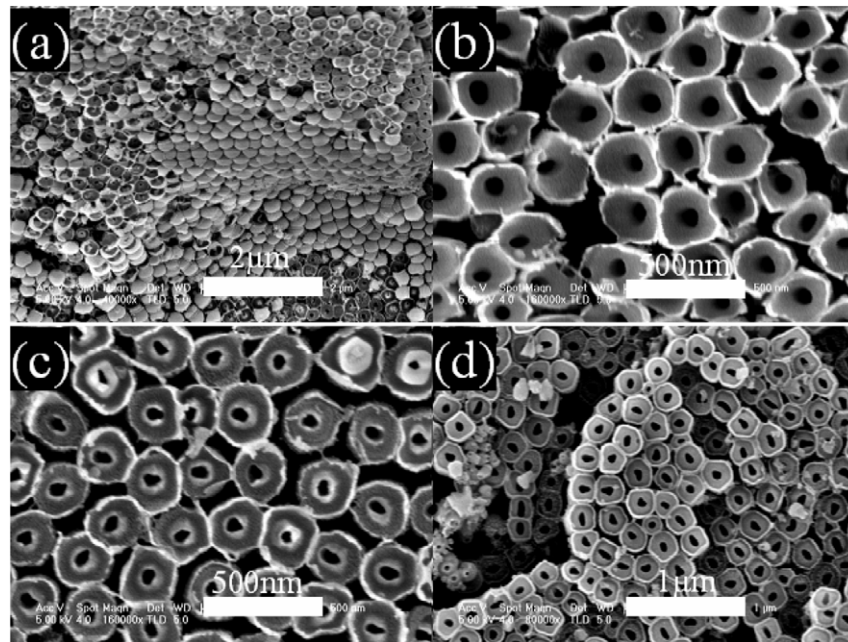


Figure 4. FESEM images of backside of TiO₂ nanotubular array membrane made from annealed titanium foils at 220 V. (a) Barrier layer still adhered to the membrane in some concave areas; (b)–(d) different areas at the backside of this membranes.

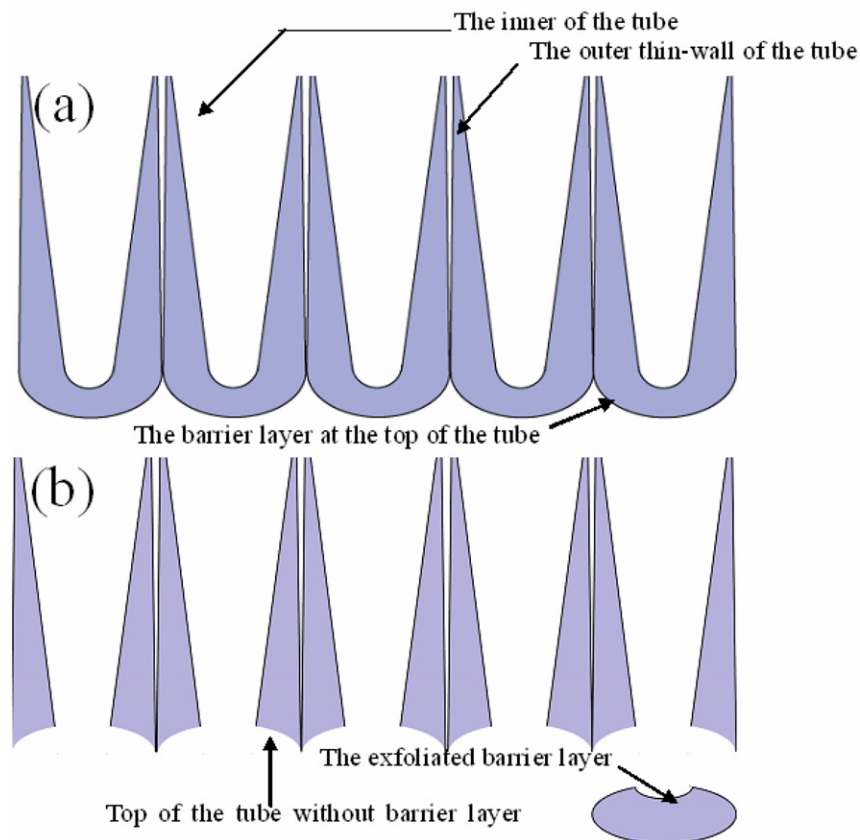


Figure 5. Schematic representation of the tube with V-like hollow structure.

(first-step anodization) made from annealed titanium exhibits a uniform pore size and ordered pore arrangement over a large area compared to that of the unannealed foil (figure 1(a)) and

the side wall of each pore decreased. Therefore, highly ordered etch pits with a thin wall on the annealed titanium foil can be realized when the oxide layer was separated completely.

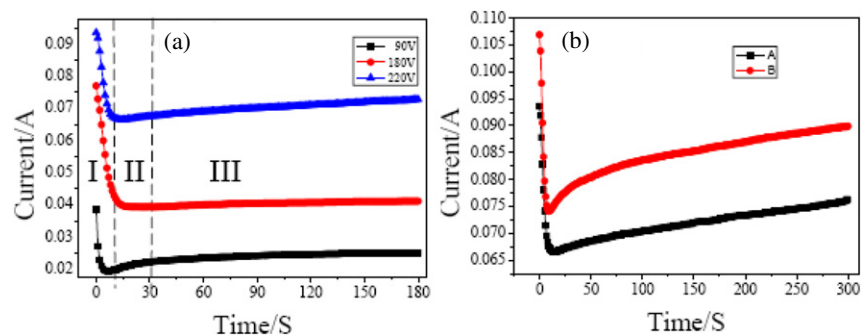


Figure 6. (a) Variation of etching current with time at different voltages at the first stage. Regions I and II are defined as unsteady states and region III is steady state; (b) variation of etching current with time at the same voltage (220 V) at the second stage for different titanium foils (curve A: unannealed titanium foils, curve B: annealed titanium foils).

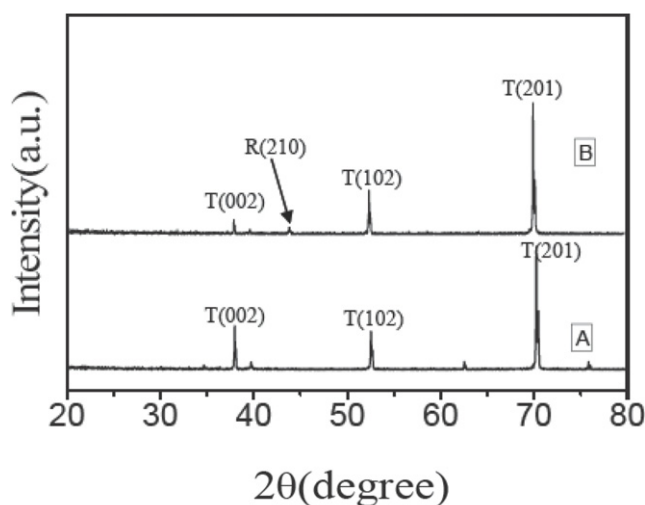


Figure 7. X-ray diffraction patterns of the two different titanium foils. A is annealed titanium foil and B is unannealed titanium foil. R and T represent rutile and titanium, respectively.

Hence, this titanium foil will be beneficial in fabricating the TiO_2 nanotubular layer with ultrathin tube walls during the second step. On the other hand, the current–time ($I-t$) curves (figure 6(b), recorded for the second step) also show that the current is larger when we used annealed titanium foils than for unannealed ones at the same voltage. This indicates that the dissolution rate of annealed foils is also larger than that of unannealed ones in the second-step anodization. Generally, a high field will lead to non-uniform distribution of hydrogen ions (reaction (2)) in each tube and these gradient-distributed electrolytes result in the formation of gradient pore diameter. Then the V-like tube forms gradually. Interestingly, the V-like structure could be formed, no matter whether the foil is annealed or unannealed. However, the V-like structure with ultrathin tube walls is not obvious enough due to its lower anodization current when the unannealed foil was used. Hence, a large current is important for fabricating this V-like structure layer with ultrathin tube walls, and an annealing process of titanium is necessary.

An annealing process of the TiO_2 membranes was further carried out for changing the morphologies and microstructures

of the TiO_2 membranes. The results indicate that at the higher annealing temperature (above 800°C) the structure of the tubes will be destroyed. Figure 8 shows the SEM upper side and backside images of the annealed TiO_2 nanotubular array membrane anodized at 220 V. It is noted that part of the barrier layer can break off from the TiO_2 membrane after annealing and the double-pass tube structures can be obtained, as shown in figures 8(a) and (d). However, membranes fabricated at a lower anodization voltage (90 V) would not produce double-pass tube structures after annealing. This indicates that the change in internal stress in the TiO_2 nanotubular array membrane during annealing at a certain high temperature is the crucial point for the formation of double-pass tube structures. This implies that an annealing process of the TiO_2 nanotubular array membranes fabricated by high-field anodization is also an effective approach to remove the barrier layer and obtain double-pass TiO_2 nanotubes.

4. Conclusion

We have prepared highly ordered TiO_2 porous membranes by two-step electrochemical oxidation under a stable high field, and the growth rate has improved greatly. A large current is important for fabricating this V-like structure layer with ultrathin tube walls. An annealing process will promote the barrier layer removal from the surface of the TiO_2 nanotube array membranes automatically, and monodisperse tubes with a double-pass structure can be fabricated. This work provides an approach to improve the morphologies and microstructures of TiO_2 nanotube arrays.

Acknowledgments

This work was supported by the Natural Science Foundation of China (grant no. 10874115), the National Major Basic Research Project of 2010CB933702, the Shanghai Nanotechnology Research Project of 0952nm01900, the Shanghai Key Basic Research Project of 08JC1411000 and the Research fund for the Doctoral Program of Higher Education of China.

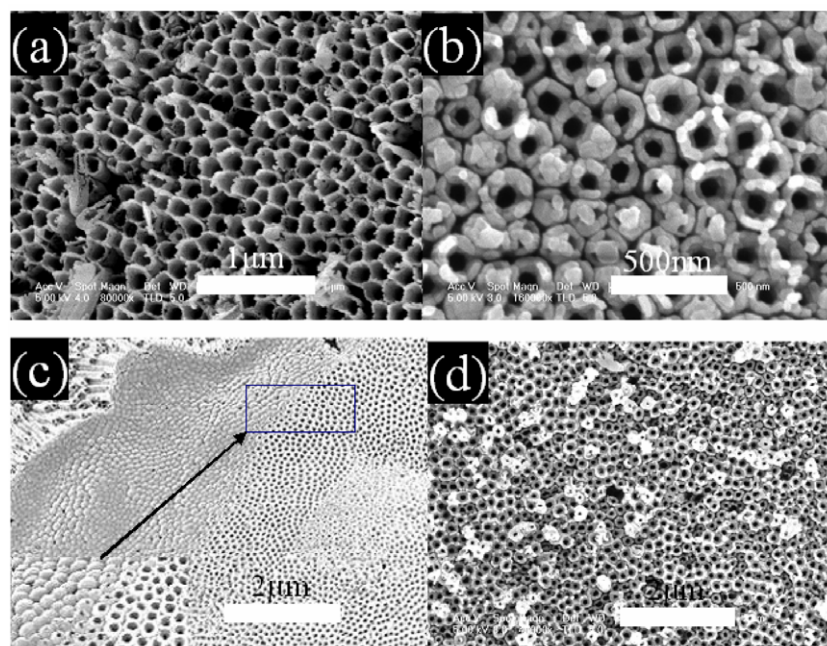


Figure 8. FESEM images of TiO₂ nanotubular array membrane annealed at 800 °C (anodic voltage: 220 V). (a) The surface images of the membrane; (b)–(d) backside images at different areas of the membranes (figure on lower left side in (c) is a higher magnification of the box).

References

- [1] Kuchibhatla S V N T, Karakoti A S, Bera D and Seal S 2007 *Prog. Mater. Sci.* **52** 699
- [2] Mor G K, Varghese O K, Paulose M, Shankar K and Grimes C A 2006 *Sol. Energy Mater. Sol. Cells* **90** 2011
- [3] Ghicov A and Schmuki P 2009 *Chem. Commun.* **2791**
- [4] Seo M H, Yuasa M, Kida T, Huh J S, Shimanoe K and Yamazoe N 2009 *Sensors Actuators B* **137** 513
- [5] O'Regan B and Grätzel M 1991 *Nature* **353** 737
- [6] Grätzel M 2001 *Nature* **414** 338
- [7] Wang H, Yip C T, Cheng K Y, Djuricic A B, Xie M H and Leung Y H 2006 *Appl. Phys. Lett.* **89** 023508
- [8] Zhu K, Neale N R, Miedaner A and Frank A J 2007 *Nano Lett.* **7** 69
- [9] Varghese O K, Paulose M and Grimes C A 2009 *Nat. Nanotechnol.* **226** 592
- [10] Xu C K, Shin P H, Cao L L, Wu J M and Gao D 2010 *Chem. Mater.* **22** 143
- [11] Fujishima A and Honda K 1972 *Nature* **238** 37
- [12] Hofmann M R, Martin S T, Choi W and Bahnemann D W 1995 *Chem. Rev.* **95** 69
- [13] Xie Y 2006 *Adv. Funct. Mater.* **16** 1823
- [14] Macak J M, Zlamal M, Krysta J and Schmuki P 2007 *Small* **3** 300
- [15] Asahi R, Morikawa T, Ohwaki T, Aoki A and Taga Y 2001 *Science* **293** 269
- [16] Yang B, Uchida M, Kim H M, Zhang X and Kokubo T 2004 *Biomaterials* **25** 1003
- [17] Adachi M, Murata Y, Okada I and Yoshikawa Y 2003 *Electrochem. Soc.* **150** G488
- [18] Mor G K, Shankar K, Paulose M, Varghese O K and Grimes C A 2006 *Nano Lett.* **6** 215
- [19] Paulose M, Shankar K, Varghese O K, Mor G K, Hardin B and Grimes C A 2006 *Nanotechnology* **17** 1
- [20] Hoyer P 1996 *Langmuir* **12** 1411
- [21] Zhong P and Que W X 2010 *Nano-Micro Lett.* **2** 1
- [22] Chen Q, Zhou W Z, Du G H and Peng L H 2002 *Adv. Mater.* **14** 1208
- [23] Yao B D, Chan Y F, Zhang X Y, Zhang W F, Yang Z Y and Wang N 2003 *Appl. Phys. Lett.* **82** 281
- [24] Jung J H, Kobayashi H, Bommel K J C, Shinkai S and Shimizu T 2002 *Chem. Mater.* **14** 1445
- [25] Kobayashi S, Hamasaki N, Suzuki M, Kimura M, Shirai H and Hanabusa K 2002 *J. Am. Chem. Soc.* **124** 6550
- [26] Boehme M, Fu G, Lonescu E and Ensinger W 2010 *Nano-Micro Lett.* **2** 26
- [27] Gong D, Grimes C A, Varghese O K, Hu W, Singh R S, Chen Z and Dickey E C 2001 *J. Mater. Res.* **16** 3331
- [28] Cai Q, Paulose M, Varghese O K and Grimes C A 2005 *J. Mater. Res.* **20** 230
- [29] Ruan C, Paulose M, Varghese O K, Mor G K and Grimes C A 2005 *J. Phys. Chem. B* **109** 15754
- [30] Macak J M, Tsuchiya H and Schmuki P 2005 *Angew. Chem. Int. Edn* **44** 2100
- [31] Macak J M, Tsuchiya H, Taveira L, Aldabergerova S and Schmuki P 2005 *Angew. Chem. Int. Edn* **44** 7463
- [32] Mor G K, Shankar K, Paulose M, Varghese O K and Grimes C A 2005 *Nano Lett.* **5** 191
- [33] Patermarakis G and Moussoutzanis K 1995 *J. Electrochem. Soc.* **142** 737
- [34] Zwilling V, Darque-Ceretti E, Boutry-Forveille A, David D, Perrin M Y and Aucouturier M 1999 *Surf. Interface Anal.* **27** 629
- [35] Beranek R, Hildebrand H and Schmuki P 2003 *Electrochem. Solid-State Lett.* **6** B12
- [36] Thompson G E, Furneaux R C, Wood G C, Richardson J A and Goode J S 1978 *Nature* **272** 433
- [37] Macak J M, Sirotna K and Schmuki P 2005 *Electrochem. Acta* **50** 3679
- [38] Taveira L V, Macak J M, Tsuchiya H, Dick L F P and Schmuki P 2005 *J. Electrochem. Soc.* **152** B405
- [39] Ghicov A, Tsuchiya H, Macak J M and Schmuki P 2005 *Electrochem. Commun.* **7** 505
- [40] Tsuchiya H, Macak J M, Taveira L, Balaur E, Ghicov A and Sirotna K 2005 *Electrochem. Commun.* **7** 576
- [41] Paulose M 2006 *J. Phys. Chem. B* **110** 16179

- [42] Paulose M, Prakasam H E, Varghese O K, Peng L, Popat K C, Mor G K, Desai T A and Grimes C A 2007 *J. Phys. Chem. C* **111** 14992
- [43] Paulose M, Peng L, Popat K C, Varghese O K, Latempa T J, Bao N Z, Desai T A and Grimes C A 2008 *J. Membr. Sci.* **319** 199
- [44] Wang J and Lin Z Q 2009 *J. Phys. Chem. C* **113** 4026
- [45] Isimjan T T, Ruby A E, Rohani S and Ray A K 2010 *Nanotechnology* **21** 055706
- [46] Li Y B, Zheng M J, Ma L and Shen W Z 2006 *Nanotechnology* **17** 5101
- [47] Nagaura T, Takeuchi F and Inoue S 2008 *Electrochim. Acta* **53** 2109
- [48] Sul Y T, Johansson C B, Jeong Y and Albrektsson T 2001 *Med. Eng. Phys.* **23** 329
- [49] Lai Y K, Sun L, Zuo J and Lin C J 2004 *Acta Phys.-Chim. Sin.* **20** 1063
- [50] Li A P, Müller F, Birner A, Nielsch K and Gösele U 1998 *J. Appl. Phys.* **84** 6023
- [51] Jessensky O, Müller F and Gösele U 1998 *Appl. Phys. Lett.* **72** 1173